Journal of the European Ceramic Society 41 (2021) 7862–7867

Contents lists available at ScienceDirect

Journal of the European Ceramic Society

journal homepage: www.elsevier.com/locate/jeurceramsoc

Crystallization of glasses – When to use the Johnson-Mehl-Avrami kinetics?

Roman Svoboda

Department of Physical Chemistry, University of Pardubice, Studentska 573, 532 10 Pardubice, Czech Republic

ARTICLE INFO

Keywords:
JMA model applicability
Theoretical simulation
Kinetic prediction

ABSTRACT

Applicability of the Johnson-Mehl-Avrami (JMA) model was tested based on the universal criterion of the kinetic peak asymmetry. Theoretical simulations were used to prepare variety of kinetic peaks with different asymmetries, which were described by the JMA model and the masterplot function z(α). Based on the correlation between the simulated crystallization peaks and the JMA description, the following intervals of the degrees of conversion corresponding to the z(α) function maxima can be attributed to the respective values of the correlation coefficients: $\alpha_{max,z} = 0.620 - 0.665$ corresponds to the better correlation with the JMA model than $r^2 = 0.999$; $\alpha_{max,z} = 0.585 - 0.705$ indicates the correlation better than $r^2 = 0.995$. These intervals are significantly more lenient than those proposed in the original derivation of the masterplot approach. Even at $r^2 = 0.995$ the fit by the JMA model provides very accurate kinetic predictions utilizable for preparation of glass-ceramics.

1. Introduction

The Johnson-Mehl-Avrami-(Kolmogorov) equation [1–5] belongs among the most famous expressions the glass scientists are familiar with. The model, usually abbreviated JMA, KJMA or JMAK (abbreviation JMA will be used in the present paper as it is the most common one), was derived to describe the macroscopic rate of crystallization in the glassy material. In particular, the formula describes the time evolution of the transformed fraction of the material α:

$$\alpha = 1 - \exp(-Kt^m) \quad (1)$$

where K is a rate constant determined by the nucleation and growth rates, and m is the Avrami exponent reflecting the growth dimensionality. The expression was derived based on the so-called extended volume concept, i.e. the volume of the reaction/transformation product that would be created if the material consisted entirely of the initial untransformed phase; the following conditions were assumed during the derivation:

a) nucleation (either homogeneous or heterogeneous) producing nuclei randomly dispersed throughout the amorphous phase
b) growth rate depends only on temperature, not on time or degree of transformation
c) crystal growth is isotropic

It has been shown in [6,7] that the applicability of the JMA equation can be extended to non-isothermal conditions, if the majority of the nuclei are formed before or during the initial stages of the crystallization process.

Due to its simplicity, physically meaningful interpretation, and lack of competing physico-chemical models suitable for the description of the crystallization behavior, the JMA equation became immensely popular. Popularity of the JMA formalism is well evidenced by the cross-search in scientific literature databases: 286 references to the "JMA AND crystallization" in Web of Science, 311 in Scopus, 1265 in Science Direct. In fact, the JMA equation is in practice one of just two solid-state models regularly used to describe the nucleation-growth based processes (with the other being the empirical Šesták-Berggren autocatalytic model [8]). The wide spread and popularity of the JMA equation led, however, to its overuse, and it is nowadays commonly applied even in cases when the base conditions for its usage are not fulfilled. In particular, the Avrami exponent *m* is often evaluated based on the so-called double-logarithm function [9–11]:

$$\frac{d\ln[-\ln(1-\alpha)]}{d(1/T)} = -\frac{m \cdot E}{R} \quad (2)$$

without verification of the JMA model suitability/applicability (in Eq. 2, *E* is the apparent activation energy of the process, *R* is the universal gas constant, and *T* is temperature). Out of the randomly selected 50 recently published papers utilizing the JMA evaluation, only the following ones used the JMA model properly and verified its applicability - [12–22]. Actual verification of the physico-chemical conditions

E-mail address: roman.svoboda@upce.cz.

https://doi.org/10.1016/j.jeurceramsoc.2021.08.026
Received 10 July 2021; Received in revised form 4 August 2021; Accepted 15 August 2021
Available online 18 August 2021

(as listed above), for which the JMA formalism was derived, is rather complicated and laborious, and requires extensive microscopic analysis. Therefore, a substitute in the form of mathematical/kinetic verification has been adopted. The (unfortunately) more popular way of verification is based on the linearity of data evaluated using Eq. 2, which however can often produce linear dependence also in cases when the usage of JMA model is not valid.

The second way of verification is represented by a direct fit of the experimental data (often obtained by the thermoanalytical techniques such as DSC or DTA) by the JMA model – this solution is the most accurate but requires a specialized software or pre-programmed spreadsheet calculation based on the following kinetic equation:

$$\Phi = \Delta H \cdot A \cdot e^{-E/RT} \cdot m(1-\alpha)[-\ln(1-\alpha)]^{1-(1/m)} \quad (3)$$

where Φ is the heat flow (measured e.g. by DSC), ΔH is the crystallization enthalpy, and A is the pre-exponential factor. Note that the product of the first three right-hand terms is denoted as the rate constant K(T), whereas the fourth right-hand term is denoted as the kinetic model function f(α). The latter has been obtained by derivation of Eq. 1 with respect to t.

The third way of the JMA model applicability verification is based on usage of the masterplots [23,24]. The JMA model has a specific asymmetry, for which the product of f(α) and g(α) (i.e. integral form of f(α)) yields maximum at α = 0.632. Of course, due to the unidealities of the experimental data, certain variance interval needs to be allowed for the JMA verification procedure. This interval was proposed to be ± 0.01 (i.e. 0.62 – 0.64) in [25] and ± 0.02 (i.e. 0.61 – 0.65) in [26]. However, the recent practice has shown (see e.g [27].) that the JMA model can be reasonably applied in much broader interval of the α values corresponding to the f(α)·g(α) maxima. Aim of the present paper is to provide, using theoretical simulations, a statistical background for the decision regarding the applicability of the JMA model.

2. Results

The fundamental outline of the present calculations is the following: the flexible Šesták-Berggren (AC) model [8] will be used to simulate variety of kinetic peaks with different asymmetries that will be consequently analyzed with respect to their easily quantifiable features (e.g. asymmetry, masterplot characteristic) and fit by the JMA model. Based on the correlation coefficient associated with the JMA fit, the suitable ranges of the general kinetic peak characteristics (asymmetry, masterplot characteristic) will be determined and attributed to the particular JMA fit accuracies.

To produce different peak asymmetries, the universal Šesták-Berggren model was implemented into the standard kinetic equation:

$$\Phi = \Delta H \cdot A \cdot e^{-E/RT} \cdot \alpha^{M}(1-\alpha)^{N} \quad (4)$$

where M and N are the kinetic exponents of the AC model. The theoretical simulations based on Eq. 4 were performed with the following parameters – $\Delta H = 1$, $\ln(A/s^{-1}) = 35$, E = 120 kJ mol^{-1}, Δα used in the integration-based simulation was 10^{-4}. Combinations of the following AC exponents values were used to cover the whole relevant range of asymmetries "close" to that of the JMA model: M = 0.25, 0.50, 0.75 and 1.00; N = 0.05–2.50 with the step of 0.05 (the step of 0.1 was used in case of the combinations with M = 1 to identify the influence of the step size on the resolution of the resulting dependences). In total, 175 AC peaks were simulated – Fig. 1 depicts examples of the simulated AC kinetic peaks to demonstrate the changes of the peak shape and position with evolution of the particular kinetic exponents.

In the first step, all simulated AC kinetic peaks were fit using the Fraser-Suzuki (FS) function [28,29] to determine the asymmetry of these peaks. Note that the mathematic FS function was shown to very well express the JMA kinetics [30] and the function is generally well suited for the description of the solid-state kinetic data [31]. The FS function is represented by Eq. 5:

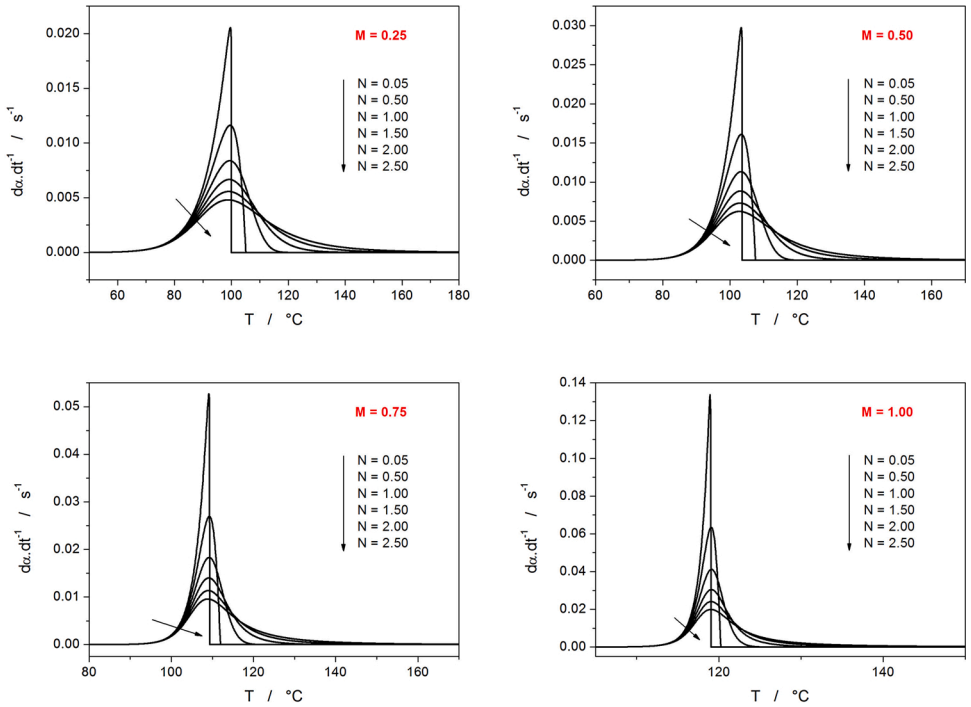

Fig. 1. Example AC kinetic peaks simulated using Eq. 4 with the following parameters: $q^{+} = 10$ °C·min^{-1}, $H = 1$, $\ln(A/s^{-1}) = 35$, E = 120 kJ·mol^{-1}, M and N exponents are indicated in the respective graphs, Δα used in the integration-based simulation was 10^{-4}. The ranges of N values cover all asymmetries explored in the present paper.

$$y = a_0 \exp\left[-\ln 2 \left[\frac{\ln\left(1 + 2a_3 \frac{x-a_1}{a_2}\right)}{a_3} \right]^2 \right] \quad (5)$$

where a_0, a_1, a_2 and a_3 are the parameters corresponding to the amplitude, position, half-width and asymmetry of the curve, respectively. Whereas the amplitude, position and half-width of the kinetic peaks are non-specific parameters with respect to the given kinetics, the value of the asymmetry parameter a_3 can be attributed to the particular kinetic models. Asymmetry of the simulated AC kinetic peaks (expressed via the a_3 coefficient of the FS function) is shown in Fig. 2A. Note that the value $a_3 = 0$ corresponds to the perfectly symmetrical peak, negative and positive asymmetries correspond to the peaks skewed to higher and lower T values, respectively. The meaningfulness of the attribution of asymmetry to the simulated AC data was tested based on the correlation coefficient of the FS fits r_{FS} – as displayed in Fig. 2B. The high correlation of the FS fits with the actual AC kinetic peaks (absolute majority of the data had $r > 0.995$) confirms the validity of the a_3 parameters attribution to the particular AC peaks. Note that the actual correspondence between the a_3 parameter and the true asymmetry of the simulated AC peaks is significantly higher than suggested by the r values, because the correlation coefficients express the conformity between the both whole curves (AC and FS), where the main deviations occur at the peak tails. Were the peak tails omitted, the correlation between the main bodies of the AC and FS curves (which actually determines the peak asymmetry) would be much higher.

In the second step (after the FS fits of the AC data), the AC kinetic peaks were fit by the JMA model (Eq. 3) – the fits were performed for the standard derivative form of the kinetic data, i.e. $d\alpha \cdot dt^{-1}$. The correlation coefficients of these fits are displayed in Fig. 3. It is apparent from Fig. 3A that only a relatively narrow range of M/N combinations used during the simulations of the AC kinetic peaks leads to the consequent acceptable description by the JMA model. Importantly, all curves for different M values used in the AC simulations that are displayed in Fig. 3A converge into one mastercurve, when (instead of the AC exponent N) they are characterized by their FS asymmetry parameter a_3 (see Fig. 3B). This indeed confirms that the JMA model has specific asymmetry: for $r = 0.999$ the a_3 interval is from -0.49 to -0.24; for $r = 0.995$ the a_3 interval is from -0.65 to -0.08. For $r^2 = 0.999$ the a_3 interval is from -0.45 to -0.28; for $r^2 = 0.995$ the a_3 interval is from -0.56 to -0.17. This indicates that in theory the fit by the FS function (with the parameter a_3 being determined in the process) could be used as a criterion for the JMA model applicability. However, since the fit of the experimental data by the FS equation is only very slightly less laborious compared to the direct fit of the data by the JMA model itself, it would not be a practical solution. Note that, as a byproduct, the values of the

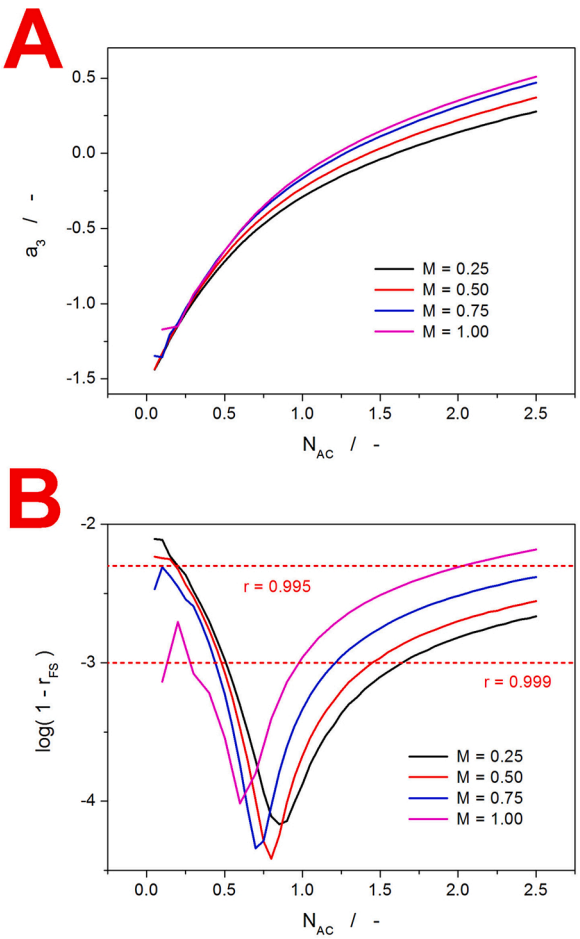

Fig. 2. A) Parameters a_3 (responsible for the peak asymmetry) of the Fraser-Suzuki function obtained during the fit of the simulated AC peaks by the FS function. B) Correlation coefficients r_{FS} obtained for the fits of the four series of the simulated AC peaks by the FS function. Dashed lines indicate the particular correlation levels between the AC model and the FS function.

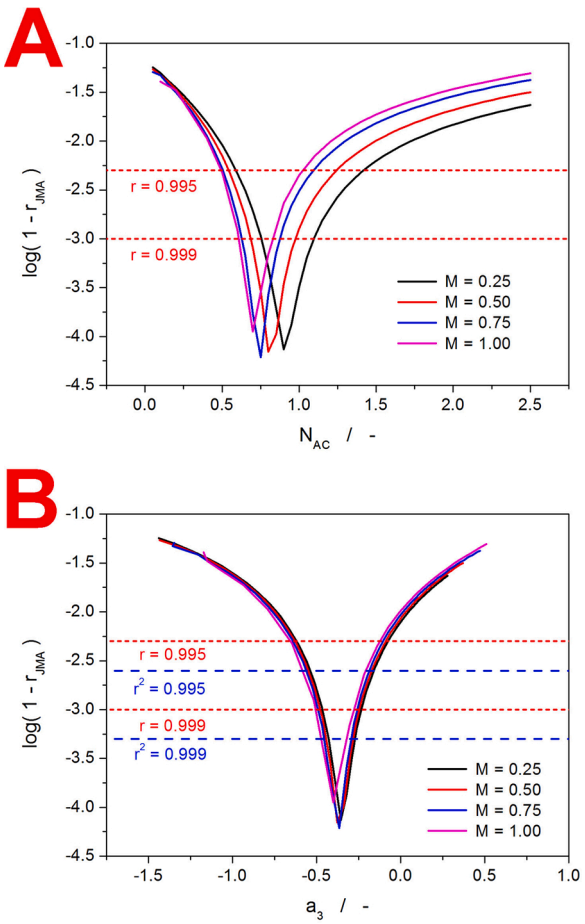

Fig. 3. A) Correlation coefficients r_{JMA} obtained for the fits of the four series of the simulated AC peaks by the JMA model. Dashed lines indicate the particular correlation levels between the AC and JMA models. The correlation coefficients are plotted against the kinetic exponent N_{AC} used in the corresponding simulation. B) Correlation coefficients r_{JMA} obtained for the fits of the four series of the simulated AC peaks by the JMA model. Dashed lines indicate the particular correlation levels between the AC and JMA models. The correlation coefficients are plotted against the Fraser-Suzuki parameter a_3 obtained during the fit of the same simulated AC peaks by the FS function.

JMA exponent *m* were obtained as a result of the fits of the various AC kinetic peaks by the JMA model – as this type of distortion and its interpretation is not the main topic of the present paper, the corresponding dependences including their discussion is published separately in the Supplemental online material.

In the third step, the AC kinetic peaks were transformed to the masterplot function z(α):

$$z(\alpha) = f(\alpha)\cdot g(\alpha) = \Phi\cdot T^2 \quad (6)$$

The α values corresponding to the maxima of these functions, $\alpha_{max,z}$, are in Fig. 4A correlated to the FS parameter a_3. The very good correlation coefficient of 0.9945 indicates that $\alpha_{max,z}$ directly reflects the asymmetry of the kinetic peaks. This finding validates the proposed universal utilization of the $\alpha_{max,z}$ value for the determination of the JMA model applicability. The statistical evaluation of the JMA model applicability is introduced in Fig. 4B, where the $\alpha_{max,z}$ values are linked to the correlation coefficients of the JMA fits to the kinetic peaks with varying asymmetry. The r = 0.999 correlation with the JMA kinetics is achieved in the interval $\alpha_{max,z}$ = 0.615 – 0.685; the r = 0.995 correlation is then achieved in the interval $\alpha_{max,z}$ = 0.535 – 0.735. For the r^2 correlations the $\alpha_{max,z}$ intervals are: 0.999 → 0.620 – 0.665; 0.995 → 0.585 – 0.705. These intervals are indeed much broader compared to the originally proposed boundaries.

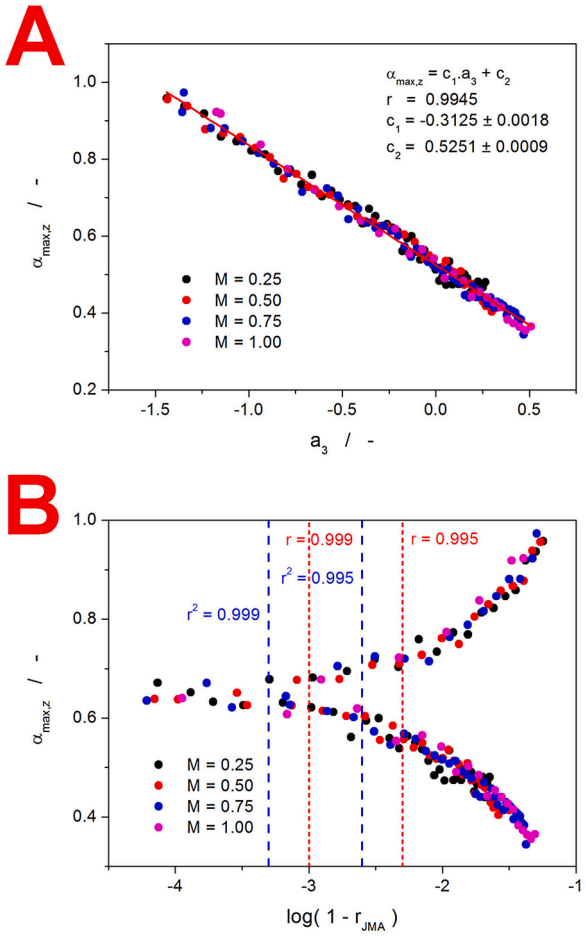

Fig. 4. A) Correlation between the $\alpha_{max,z}$ values determined directly for the simulated AC peaks, and the a_3 parameters obtained during the fit of the simulated AC peaks by the FS function. B) $\alpha_{max,z}$ values determined directly for the simulated AC peaks plotted against the correlation coefficients r_{JMA} obtained for the fits of the simulated AC peaks by the JMA model. Dashed lines indicate the particular correlation levels between the AC and JMA models.

3. Discussion

Large variety of kinetic peaks (simulated in terms of the AC model) with different asymmetries were fit by the JMA model (Eq. 3) and evaluated by means of the masterplot function z(α) (Eq. 6). In this way, the intervals for the $\alpha_{max,z}$ values were determined, for which the kinetic peak very well corresponds to the JMA kinetics. The kinetic peaks presented in Section 2 were all simulated for the $\ln(A/s^{-1}) = 35$ & $E = 120$ kJ mol^{-1} combination of model-free kinetic parameters. In order to verify the universality of the presented findings, all the calculations were repeated for two other combinations of E and A values: $\ln(A/s^{-1}) = 15.5$ & $E = 60$ kJ mol^{-1}, and $\ln(A/s^{-1}) = 60$ & $E = 200$ kJ mol^{-1}. This range of E values covers majority of the commonly encountered cases of solid-state kinetics (note that the pre-exponential factor only determines the peak position on the temperature axis and does not influence the peak asymmetry or width). As was expected, all tested combinations of E and A provided exactly similar log(1-r_{JMA})-a_3 and $\alpha_{max,z}$-log(1-r_{JMA}) dependences, which indeed confirms universality of the present findings (even outside of the above-mentioned tested E/A limits).

The correlation coefficients for the JMA fits presented in Section 2 are crucial for the practical utilization of the corresponding $\alpha_{max,z}$ intervals (see Fig. 4B). However, one needs to be able to associate these correlation coefficients with the real-life consequences in order to consider their importance. The deviations of the α-T dependences during the standard non-isothermal heating scan at 10 °C min^{-1} are shown in Fig. 5. Each graph depicts the data-curves simulated using the AC model at $\Delta H = 1$, $\ln(A/s^{-1}) = 35$, $E = 120$ kJ mol^{-1}, M as denoted in the graph, and N corresponding to the $\alpha_{max,z}$ values determined from Fig. 4B (the exact $\alpha_{max,z}$ values are mentioned at the end of section 2; the corresponding N values were calculated using the interpolation between the simulated data). The α-T dependences in Fig. 5 show that even in the case of $r^2 = 0.995$ a very reasonable description of the experimental data would be achieved using the JMA kinetics. Importantly, the deviations in the kinetic description occur at the high-α stages of the kinetic process (crystallization), and the initial onset remains under these conditions practically unaltered. This has very important consequences with respect to the main goal of the kinetic analysis, i.e. prediction of the materials behavior under extrapolated experimental conditions. The data from Fig. 5 prove that for the JMA-resembling kinetics the slight deviations arising from the usage of the JMA model for slightly different peak asymmetries still result in a very accurate determination of the onset of the process (provided that the E and A values are determined correctly and in accordance with the experimental data). This is a crucial information especially with respect to the determination of the stability of the glassy materials during their storage, processing or particular application conditions.

In addition to the non-isothermal comparison depicted in Fig. 5, the analogous simulations were performed also for the true extrapolation of the kinetic behavior – the isothermal annealing at 50 °C. The corresponding α-t dependences are shown in Fig. 6, defined similarly as in Fig. 5. Apart from the same conclusion regarding the exactly similar onset of the data even at the reported deviations from the JMA model, the isothermal dependences also show that up to ~ 70 % of material's crystallinity the deviations in the reached α are negligible, and even at the late/end stages of the crystallization process the deviations do not exceed 10 % for the $r^2 = 0.995$ correlation. This makes the JMA utilization in less-than-ideal cases also perfectly viable with respect to the production of glass-ceramics, where the exact amount of the crystalline phase in the glassy matrix would be of concern. Lastly, in the case of the preparation of fully ceramic material, the times needed to reach full crystallinity can (especially for the slowly crystallizing materials as indicated by the lower M value) vary, depending on the r^2 value, up to 30 % for the levels of correlation tested in the present paper. This means that at larger deviations from the ideal JMA behavior the crystallization times or temperatures should be increased for the procedure to certainly

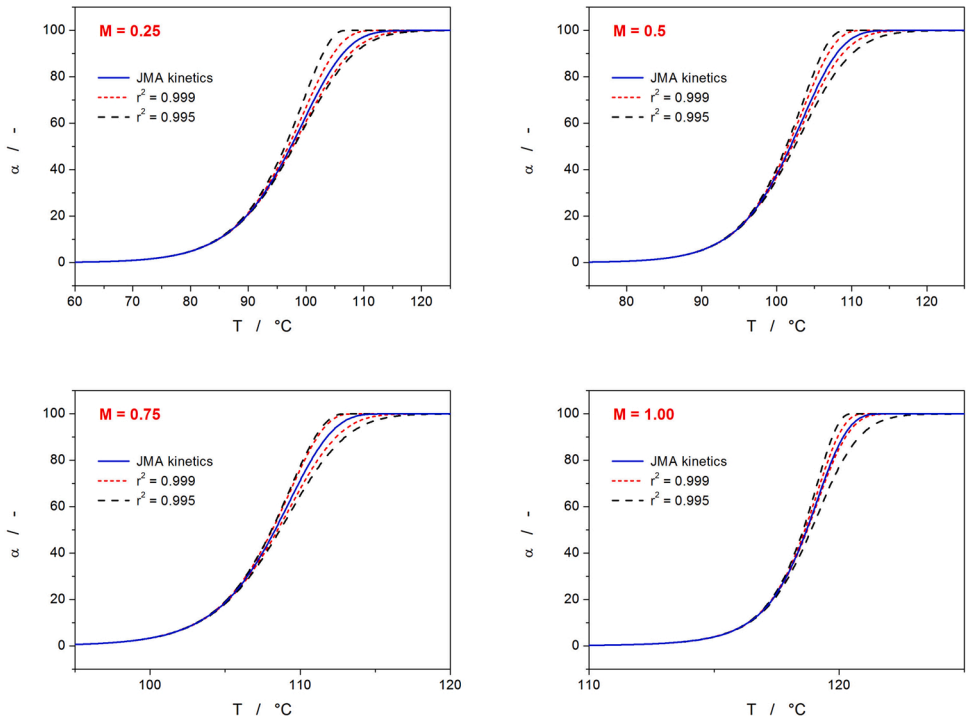

Fig. 5. Kinetic predictions for the non-isothermal heating at 10 °C·min^{-1} simulated in terms of the AC kinetics corresponding to the different correlations with the JMA model – as derived from Fig. 4B.

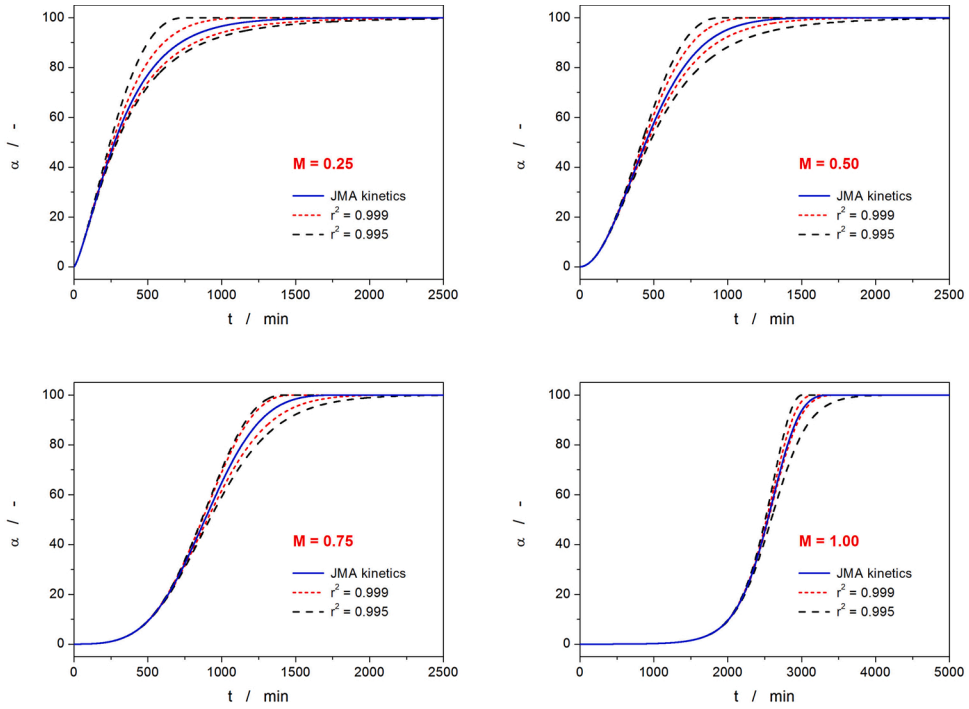

Fig. 6. Kinetic predictions for the isothermal annealing at 50 °C simulated in terms of the AC kinetics corresponding to the different correlations with the JMA model – as derived from Fig. 4B.

produce the fully crystalline material.

4. Conclusions

Kinetic peaks with different asymmetry were simulated in terms of the autocatalytic kinetics, and consequently fit by the JMA model. Based on the correlation coefficients associated with the fit by the JMA model, borderline asymmetries corresponding to the JMA kinetics were determined for the correlations $r^2 = 0.999$ and $r^2 = 0.995$. These asymmetries were consequently associated with the simple metrics of the so-called z(α) masterplot function, finding the following limits for the two respective correlation boundaries: $\alpha_{max,z} = 0.620 - 0.665$ for $r^2 = 0.999$, and $\alpha_{max,z} = 0.585 - 0.705$ for $r^2 = 0.995$. These ranges are universally valid and significantly broader compared to the original

limits of the JMA model applicability proposed in the paper that introduced the z(α) masterplot function. It was further shown that also in the case of the correlation coefficient of $r^2 = 0.995$ between the experimental data and the fit by the nucleation-growth JMA model, a very accurate kinetic prediction (even extrapolated far outside the range of the measured experimental data) would be achieved. The predicted crystallization signals had exactly similar onsets, which validates the utilization of the new JMA applicability limits for all glass-stability tests. In addition, the predicted degree of achieved crystallinity was practically unaltered up to 70 %, which approves such data for usage in preparation of the glass-ceramics.

Declaration of Competing Interest

The authors report no declarations of interest.

Acknowledgment

This work has been supported by the grant LM2018103 from the Ministry of Education, Youth and Sports of the Czech Republic.

Appendix A. Supplementary data

Supplementary material related to this article can be found, in the online version, at doi:https://doi.org/10.1016/j.jeurceramsoc.2021.08.026.

References

[1] W.A. Johnson, K.F. Mehl, Reaction kinetics in processes of nucleation and growth, Trans. Am. Inst. Min. (Metall) Eng. 135 (1939) 416–442.
[2] M. Avrami, Kinetics of phase change I–general theory, J. Chem. Phys. 7 (1939) 1103–1112.
[3] M. Avrami, Kinetics of phase change. II–transformation-time relations for random distribution of nuclei, J. Chem. Phys. 7 (1940) 212–224.
[4] M. Avrami, Granulation, phase change, and microstructure – kinetics of phase change III, J. Chem. Phys. 7 (1941) 177–184.
[5] A.N. Kolmogorov, On the statistical theory of the crystallization of metals, Bull. Acad. Sci. USSR 1 (1937) 355–359.
[6] D.W. Henderson, Experimental analysis of nonisothermal transformation involving nucleation and growth, J. Therm. Anal. 15 (1979) 325–331.
[7] D.W. Henderson, Thermal analysis of non-isothermal crystallization kinetics in glass forming liquids, J. Non-Cryst. Sol. 30 (1979) 301–315.
[8] J. Šesták, Thermophysical Properties of Solids, Their Measurements and Theoretical Analysis, Elsevier, Amsterdam, 1984.
[9] K. Matusita, T. Komatsu, R. Yokota, Kinetics of non-isothermal crystallization process and activation energy for crystal growth in amorphous materials, J. Mater. Sci. 19 (1984) 291–296.
[10] A.W. Coats, J.P. Redfern, Kinetic parameters from thermogravimetric data, Nature 201 (1964) 58–69.
[11] J. Šesták, On the applicability of the p(x)-function to the determination of reaction kinetics under non-isothermal conditions, Thermochim. Acta 3 (1971) 150–154.
[12] A.A. Joraid, A.S. Solieman, M.A. Al-Maghrabi, M.H. Almutairy, Studies of crystallization kinetics and optical properties of ZnO films prepared by sol–gel technique, J. Sol-Gel Sci. Technol. 97 (2021) 523–539.
[13] A.K. Diab, M.M. Abd El-Raheem, E.R. Shaaban, H.M. Ali, M.M. Wakkad, Y.A. Taya, E.S. Yousef, Crystallization kinetics of $Pb_{12}Ge_{12}Se_{76}$ chalcogenide glass, Phase Transit. 93 (2020) 323–337.
[14] F. Baino, E. Fiume, Quantifying the effect of particle size on the crystallization of 45S5bioactive glass, Mat. Lett. 224 (2018) 54–58.
[15] T. Paul, G. Mountjoy, A. Ghosh, Thermal and structural investigations of xLi2O-(1-x)Bi2O3(0.25 ≤ x ≤ 0.35) glasses, Int. J. Appl. Glass Sci. 9 (2018) 319–332.
[16] R. Golovchak, A. Kozdras, T. Hodge, J. Slezak, C. Boussard-Pledel, Ya Shpotyuk, B. Bureau, Optical and thermal properties of Sb/Bi-modified mixed Ge-Ga-Se-Te glasses, J. Alloys Compd. 750 (2015) 721–728.
[17] X. Wang, J. Pang, L.Y. Guo, H.J. Ma, K.B. Kim, W.M. Wang, Thermal analysis of directional pressure annealed Fe78Si9B13 amorphous ribbons, Thermochim. Acta 661 (2018) 67–77.
[18] E.B. Peixoto, E.C. Mendonca, S.G. Mercena, A.C.B. Jesus, C.C.S. Barbosa, C. T. Meneses, J.G.S. Duque, R.A.G. Silva, Study of the dynamic of crystallization of an amorphous Fe40Ni40P14B6 ribbon through Johnson-Mehl-Avrami model, J. Alloys Compd. 731 (2018) 1275–1279.
[19] B. Pan, L. Dang, Z. Wang, J. Jiang, H. Wei, Preparation, crystal structure and solution-mediated phase transformation of a novel solid-state form of CL-20, CrystEngComm 20 (2018) 1553–1563.
[20] M. Mohamed, A.M. Abd-Elnairem, R.M. Hassan, M.A. Abdel-Rahim, M.M. Hafiz, Non-isothermal crystallization kinetics of As30Te60Ga10 glass, Appl. Phys. A 123 (2017) 511.
[21] Z. Liu, J. Xu, Y. Wang, Z. Jian, J. Liu, Calorimetric studies on Ge23Se67Sb10-0.5% RbI glass, Optik 142 (2017) 529–535.
[22] Z. Jamili-Shirvan, M. Haddad-Sabzevar, J. Vahdati-Khaki, K.-F. Yao, Thermal behavior and non-isothermal crystallization kinetics of (Ti41Zr25Be28Fe6)93Cu7 bulk metallic glass, J. Non-Cryst. Sol. 447 (2016) 156–166.
[23] S. Vyazovkin, A.K. Burnham, J.M. Criado, L.A. Pérez-Maqueda, C. Popescu, N. Sbirrazzuoli, ICTAC Kinetics Committee recommendations for performing kinetic computations on thermal analysis data, Thermochim. Acta 520 (2011) 1–19.
[24] J. Malek, The kinetic-analysis of nonisothermal data, Thermochim. Acta 200 (1992) 257–269.
[25] J. Málek, The applicability of Johnson-Mehl-Avrami model in the thermal analysis of the crystallization kinetics of glasses, Thermochim. Acta 267 (1995) 61–73.
[26] J. Málek, Kinetic analysis of crystallization processes in amorphous materials, Thermochim. Acta 355 (2000) 239–253.
[27] R. Svoboda, J. Málek, Interpretation of crystallization kinetics results provided by DSC, Thermochim. Acta 526 (2011) 237–251.
[28] R.D.B. Fraser, E. Suzuki, Resolution of overlapping absorption bands by least squares procedures, Anal. Chem. 38 (1966) 1770–1773.
[29] R.D.B. Fraser, E. Suzuki, Resolution of overlapping bands – functions for simulating band shapes, Anal. Chem. 61 (1969) 37–39.
[30] R. Svoboda, J. Málek, Applicability of Fraser-Suzuki function in kinetic analysis of complex processes, J. Therm. Anal. Cal. 111 (2013) 1045–1056.
[31] A. Perejón, P.E. Sánchéz-Jiménez, J.M. Criado, L.A. Pérez-Maqueda, Kinetic analysis of complex solid-state reactions. A new deconvolution procedure, J. Phys. Chem. B 115 (2011) 1780–1791.